Cynara cardunculus L. gasification in a bubbling fluidized bed: The effect of magnesite and olivine on product gas, tar and gasification performance

Daniel Serrano[a]*, Marzena Kwapinska[b]*, Alen Horvat[c], Sergio Sánchez Delgado[a], James J. Leahy[c]

[a] *Carlos III University of Madrid, Energy Systems Engineering Group, Thermal and Fluid Engineering Department. Avda. de la Universidad 30, 28911 Leganés (Madrid), Spain*

[b] *Technology Centre for Biorefining and Biofuels, University of Limerick, Limerick, Ireland*

[c] *Carbolea Research Group, Department of Chemical and Environmental Sciences, University of Limerick, Limerick, Ireland*

*T: +34916248884; E-mail: daserran@ing.uc3m.es

*T: +35361 233290; E-mail: marzena.kwapinska@ul.ie

Abstract

Gasification of *Cynara cardunculus* L. was performed in a bubbling fluidized bed (BFB) using air as the gasifying agent and magnesite and olivine as different bed materials. Temperature was varied during the experiments (700-800 ºC) with fixed biomass feeding and air flow rates. The effect of using the magnesite and olivine on the gas and tar composition, carbon and biomass conversion, and cold gas efficiency was investigated. The product gas showed high hydrogen content (13-16 %v/v) for both magnesite and olivine in the temperature range studied. Higher heating value and gas yield were improved with increasing the temperature from 700 to 800 ºC. Biomass and carbon conversion were greater than 75%, giving values higher than 90 % for both 700 and 800 ºC in magnesite and for 800 ºC in olivine. Indane and cresols were the main tar compounds at low temperature while naphthalene was the dominant tar species at the high temperatures. Gasification performance was better with magnesite at 700 ºC while olivine showed better properties at 800 ºC.

Keywords

C. cardunculus L., biomass, gasification, fluidized bed, tar

1. Introduction

Gasification is a thermochemical process that transforms different carbonaceous materials like biomass into a useful product gas or chemical feedstock [1]. The process needs a small amount of oxygen, less than that required for stoichiometric oxidizing conditions, to produce a combustible gas composed of H_2, CO, CH_4, CO_2, N_2 and light hydrocarbons, with limited formation of dioxins, SO_x and NO_x, as NH_3 and H_2S are the main nitrogen and sulphur compounds formed due to the reducing conditions during gasification [2]. The flexibility in terms of feedstock type and size, the good solid-gas mixing and temperature control, and high mass transfer rate, make bubbling fluidized bed (BFB) reactors an advantageous option for biomass gasification [3,4]. However, there are two key considerations to be taken into account in biomass gasification in a BFB reactor; the high alkali content in biomass and tar production. The high alkali content promotes bed agglomeration changing the operating conditions and leading in some cases to defluidization. Tars, previously defined by Milne et al. [5] as the organics produced under thermal or partial-oxidation regimes of any organic material and generally assumed to be largely aromatic, and defined by Kiel et al. [6] as all organic compounds with a molecular weight larger than benzene, excluding soot and char, also need to be considered. Tar related issues can lead to unscheduled stops and may impact the performance of downstream unit processes [7].

The potential end use of the product gas is determined by the tar composition and concentration: gas compression for transport in pipework imposes an upper tar limit of less than 600 mg/Nm^3; the maximum tar concentration for internal combustion engines is 100 mg/Nm^3, with phenols and cresols in particular considered corrosive for internal combustion engines; less than 0.1 mg/Nm^3 is required for synthesis applications. However in the case of close-couple combustors, the gas quality is not a major issue. Different cleaning technologies, ranging from cyclones, coolers, filters or catalytic cracking or reforming, are available to condition the gas characteristics in order to meet the specific requirements of the selected application [5].

Different bed materials such as dolomite, magnesite, olivine or metal based catalysts are frequently used in order to avoid agglomeration, to reduce tar yield and to improve gas composition [8,9]. Corella et al. [10] compared dolomite and olivine, concluding that dolomite was better for tar reduction but generated more fine particles than olivine. Many authors have studied the performance of olivine as an in-bed catalyst with different types of feedstock such as woody biomass or plastic waste, obtaining improvements in gas composition and tar yield compared to silica sand [11–13]. Rapagnà et al. [14] used olivine particles during steam gasification of almond shells, concluding that it had good catalytic activity at temperatures around 800 ºC. Magnesite is another alternative as a bed material in BFB gasification. Siedlecki et al. [7] obtained very promising results using magnesite either as a bed additive or as a bed material. In addition to bed material,l gasification conditions such as temperature, biomass type and throughput, gasifying agent or gasifier configuration also affect tar yield and gas composition [15]. Gasification temperatures between 700 and 800 ºC are critically important in terms of tar mitigation as they are high enough to produce limited quantities of tar while below the dew point of many tar molecules [16].

Cardoon or thistle can be a good option for biomass gasification compared with other energy crops due to its low cost, their low nitrogen pollution, low water consumption, it can be cultivated on land unsuitable for food production and it enhances soil characteristics [17,18]. It is a herbaceous perennial species well adapted to Mediterranean regions with hot dry summers [18]. Among the Mediterranean countries, Spain has ideal conditions for cardoon production [19], moreover, the biomass from this plant has high volatile matter content (>75%), which is an important benefit in biomass gasification [20]. The interest in this energy crop is not new, Herguido et al. [21] gasified different biomasses in a BFB with steam, including *C. cardunculus*, studying the effect of temperature on gas composition, char and tar yields using silica sand as the bed material. Their results showed both low gas yield and carbon conversion, and high char yield. Steam gasification of cardoon was also studied by Encinar et al. [22] and the results were compared with cardoon pyrolysis in a fixed bed reactor under similar conditions

[20]. They reported that H_2 yield was better for steam gasification than for pyrolysis at the same temperature. High temperature favoured the generation of H_2 and CO, as well as gas yield and conversion rates. Zabaniotou et al. [19] gasified *C. cardunculus* in a fixed bed reactor for different equivalent ratios and temperatures. They concluded that the product gas obtained by fixed bed air gasification was similar to steam gasification in terms of H_2 and CO, with high H_2 content. As a result they suggested cardoon gasification as a possible route for H_2 production.

Some investigations on combustion and gasification of thistle have recently been carried out with the goal of understanding the role of its high alkali content in bed agglomeration. Abelha et al. [23] employed blends of cardoon and eucalyptus to reduce agglomeration while gasifying with a mixture of air and steam using silica sand as the bed material. Agglomeration decreased and it finally disappeared when 80 % w/w of eucalyptus was used. However, higher amounts of H_2 and low tar content were obtained when eucalyptus was not used and cardoon was gasified on its own with air and steam. On the other hand, it was observed that dolomite prevented agglomeration even with low concentrations of eucalyptus. Similar results in terms of bed agglomeration were reported by Christodoulou et al. [24] who used giant reed in combination with *C. cardunculus*, employing magnesite and olivine as bed materials i.e. agglomeration occurred when cardoon only was gasified either with magnesite or olivine. In another study, Christodoulou et al. [25] analyzed the agglomerates obtained from gasifying cardoon in an olivine bed. The agglomerates were found to be formed by a melted phase rich in sodium, potassium, calcium, magnesium and silicon. Serrano et al. [26] used silica sand and an alternative bed material, sepiolite, in order to compare the defluidization time and agglomerates during cardoon gasification at different air velocities and observed that the sepiolite delayed the defluidization time by up to an order of magnitude compared with silica sand. These studies show that the use of different bed materials such as magnesite, olivine or sepiolite can delay agglomeration and suggest that dolomite can be used to completely avoid it. Cardoon co-gasification with other types of biomass such as woody biomass (e.g. eucalyptus or giant reed) appears to be a promising strategy to mitigate agglomeration problems. Additionally, kaolin

($Al_2Si_2O_5(OH)_4$) has been proven to be an effective additive to increase the ash melting point/temperature [27–30] and prevent or mitigate agglomeration when gasifying high alkali biomass.

As stated by Kiel et al. [6] tar analyses not only need to be focused on the amount of total tar generation (g/Nm^3) but also on its composition. When tar composition is known the tar dew point which defines its condensation behavior can be calculated and the solubility of the tar in water can be evaluated. In spite of the aforementioned studies based on cardoon gasification, only one of them [24] gives some information about tar generation and speciation. To the authors' knowledge no other studies have been reported regarding this aspect of *C. cardunculus* gasification. The present work focuses on air gasification of this biomass and examines the role of temperature (between 700 and 800 ºC), and bed materials on agglomeration using kaolin cardoon. The analysis also includes a discussion of gas composition and gasification performance. A detailed tar analysis was undertaken and the tars are evaluated in terms of total tar and the main individual compounds. Finally, a mass balance was carried out to check the consistency of the results and to obtain information for future work.

2. Experimental methodology

2.1. Biomass and bed materials characterization

The feedstock used in these experiments was *C. cardunculus* L. Proximate and ultimate analyses were carried out using a TGA Q500 thermogravimetric analyzer (TA Instruments) and a Leco TruSpec CHN-S elemental analyser. Higher heating value (HHV) was also measured with a Parr 6300 isoperibolic calorimeter. Finally, inorganic elemental composition analysis using atomic absorption spectrometer (Spectra A, 220) was performed on the biomass ash and ash collected from cyclones. All the samples were digested in H_2O_2, HNO_3, H_2SO_4 and HF prior to analysis by atomic absorption. These analyses were accomplished according to the corresponding EN standard for solid biofuels. The chemical composition of the biomass was

determined according to the procedure described in Xue et al. [31]. The results of the *C. cardunculus* L. characterization are shown in Table 1.

Biomass was received as cylindrical pellets of approximately 6 mm in diameter with lengths varying from 5 to 25 mm. These pellets were too large for the feeding system and were therefore crushed prior to gasification into particles between 1 and 5 mm with a mean particle size of 2.86 ± 0.19 mm and bulk density of 487.01 ± 28.52 kg/m^3.

Table 1. *C. cardunculus* L. characterization (cardoon ar. with 3 wt. % of added kaolin).

Proximate analysis		Ultimate analysis	
Moisture [wt % ar]	9.69	Carbon [wt. % db]	48.90
Volatile Matter [wt. % ar]	69.83	Hydrogen [wt. % db]	5.90
Fixed Carbon [wt. % ar]	10.21	Nitrogen [wt. % db]	0.57
Ash [wt. % ar]	10.27	Sulphur [wt. % db]	0.05
		Oxygen[a] [wt. % db]	33.20
Higher heating value [MJ/kg db]	17.73		
Chemical composition [wt. % db]			
Hemicellulose	17.53		
Cellulose	31.41		
Lignin	17.69		
Ethanol extractives	7.86		
Ash analysis [g/kg ash db]			
Al	122.66	Mg	20.07
Ca	167.27	Na	274.32
Cu	5.69	Si	383.60
Fe	10.37	Se	6.13
K	95.90		
Trace metals [mg/kg ash db]			
Cd	223.02	Mo	892.08
Co	245.32	Ni	458.31
Cr	111.51	Pb	11.15
Mn	563.13	Zn	345.68

ar: as received, db: dry basis, [a] by difference

C. cardunculus is known to have a relatively high ash content varying from 4.2 % to 15.4 % on a dry basis [19,23,24] when compared to other energy crops like miscanthus [31] or willow [32]. In the present study this value was 11.38 % (dry basis) including added kaolin which had been mixed with the *C. cardunculus* L (Table 1) to prevent agglomeration. Previous gasification studies had reported some agglomeration problems when gasifying this energy crop due to the high amounts of alkali metals such as K and Na [23–26]. The amount of kaolin added was 3

wt.% of the biomass loaded into the feeding system. This quantity was similar to that used by Llorente et al. [29] and Weber and Quicker [30].

Two different bed materials, magnesite and olivine, were tested in separate experiments in order to compare their catalytic effects during *C. cardunculus* L. gasification at different temperatures. These bed materials were chosen due to their lower cost than metal based catalysts, their better mechanical properties and relatively good tar reduction properties reported in literature as well as their availability due to their natural occurring nature. Magnesite ($MgCO_3$) was supplied by MINELCO, U.K. and olivine ($(Mg,Fe_2)SiO_4$) by Magnolithe, Austria. The two bed materials were sieved to between 300 and 500 μm prior to gasification and taking into account their respective densities both the magnesite and olivine corresponded to type B materials according to Geldart's classification [33]. The main properties of the bed materials are shown in Table 2.

Table 2. Magnesite and olivine properties.

	Magnesite	Olivine
Density [kg/m^3]	3207	3146
Bulk density [kg/m^3]	1358	1314
Mean particle diameter [μm]	391	407
Minimum fluidization velocity at 750 ºC [m/s]	0.085	0.082

2.2. Experimental setup

The experiments were conducted in a pilot scale air-blown bubbling fluidized bed gasifier (BFB) located in the Carbolea Research Group facilities at the University of Limerick. Figure 1 shows a diagram of the facility which consists of different sections: biomass feeding, air supply and heating, fluidized bed reactor, a downstream cleaning section with cyclones and hot gas filter, and product gas analysis. The bed section has an inner diameter (ID) of 134.5 mm with a height of 1750 mm, and the freeboard section has an ID of 211.6 mm and a height of 1250 mm. Both sections, as well as downstream pipes, cyclones and hot filter were externally heated. Air, introduced at the bottom of the reactor through a 3 mm thick perforated stainless 316 distributor

plate with 40 holes of 0.9 mm inner diameter arranged in a circular distribution was used as the gasifying medium. Biomass was fed into the gasifier 190 mm above the distributor plate by means of two screw feeders. Temperature and pressure were monitored at each section of the pilot plant. A more detailed description can be found elsewhere [34].

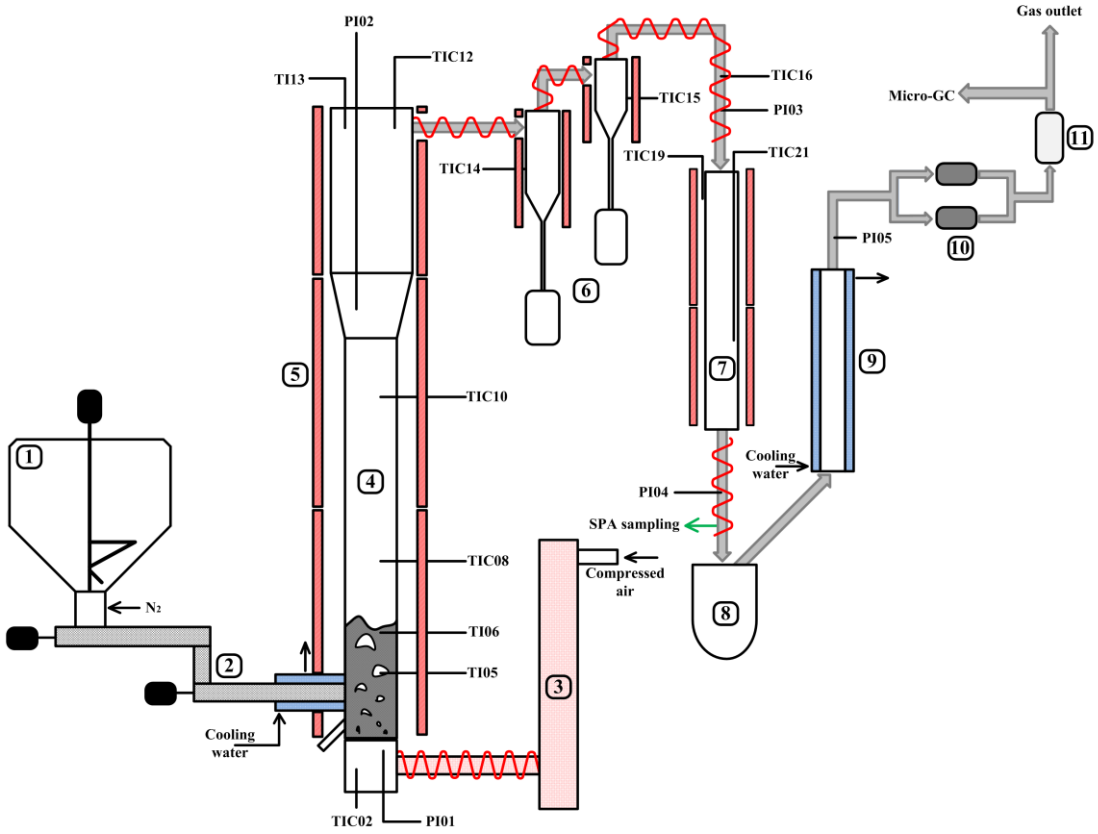

Figure 1. Schematic of the experimental facility at the University of Limerick: 1) biomass hopper; 2) screw feeders; 3) air preheater; 4) BFB reactor; 5) electrical furnaces; 6) cyclones; 7) hot filter; 8) water and tar trap; 9) heat exchanger; 10) downstream filters; 11) mass flow meter.

The minimum fluidization velocity for the different bed materials was determined prior to the gasification experiments measuring the ΔP of the bed versus the superficial gas velocity (Table 2).

2.3. Experimental procedure

Before starting each experiment, a bed aspect ratio, defined as the relation between the bed height and the reactor diameter (D), was set to $h_b/D = 2$. With this aspect ratio, the amount of bed material loaded into the reactor was 5.70 kg in the case of the magnesite experiments and 5.38 kg in the case of olivine. The air supply was turned on and set to the air flow rate for gasification, around 63 Ndm^3/min which equates to an approximate u/u_{mf} ratio of 3, a typical value for BFB gasifiers. The external electrical furnaces were set to the experiment temperature: 700, 750 or 800 ºC, and the measured experimental temperatures were close to these values. When the maximum achievable temperature in the bed using the external heating was reached, around 400-500 ºC, biomass feeding was initiated with a constant rate of around 4.5 kg/h, on an as-received basis. Under these conditions (air and biomass feed rate), the resultant equivalence ratio (ER), defined as the ratio between the O_2 introduced into the gasifier and the O_2 needed for the complete stoichometric combustion of the fuel, was kept constant at 0.20. In order to prevent backflow of the gases from the gasifier through the feeding system, a nitrogen flow of 2 Ndm^3/min was maintained from the biomass hopper to the gasifier. The exact amount of fuel fed into the reactor was obtained by weighing the mass of biomass loaded into the hopper before starting the experiment and the mass remaining inside the hopper after each test. The main operating conditions are summarized in Table 3.

Table 3. Operating conditions and syngas composition from each gasification experiment.

Operating conditions					
Bed material	magnesite	magnesite	olivine	olivine	olivine
Bed material loaded [kg]	5.70	5.70	5.38	5.38	5.38
Biomass feeding rate [kg_{daf}/h]	3.63	3.56	3.51	3.60	3.52
Biomass throughput daf [kg_{daf}/m^2h]	255.55	250.37	247.17	253.53	247.42
Air flow rate [Ndm^3/min]	63.43	63.47	62.79	63.36	63.13
ER [–]	0.20	0.20	0.20	0.20	0.20
u/u_{mf} [–]	2.91	3.06	3.01	3.19	3.35
Inlet air temperature, TIC02 [ºC]	209	270	227	276	320
Gasifcation temperature, TIC10 [ºC]	700	800	700	760	800
TI06 [ºC]	701	756	718	741	791
Syngas composition (dry)					
H_2 [% v/v]	13.48 ± 0.38	16.51 ± 0.27	12.62 ± 0.82	13.64 ± 0.36	16.26 ± 0.33
CO [% v/v]	10.01 ± 0.23	15.05 ± 0.52	10.68 ± 0.66	13.89 ± 0.40	16.71 ± 0.30
CH_4 [% v/v]	5.33 ± 0.18	4.89 ± 0.10	4.88 ± 0.06	5.29 ± 0.09	4.87 ± 0.26

CO_2 [% v/v]	17.37 ± 0.17	16.77 ± 0.07	16.98 ± 0.18	16.83 ± 0.08	16.56 ± 0.12
C_2H_4 [% v/v]	2.45 ± 0.03	2.07± 0.01	2.34 ± 0.02	2.19 ± 0.03	1.96 ± 0.03
C_2H_6 [% v/v]	0.30 ± 0.01	0.22 ± 0.00	0.00 ± 0.00	0.00 ± 0.00	0.29 ± 0.01
N_2 [% v/v]	51.07 ± 1.18	44.50 ± 0.71	52.51 ± 1.11	48.16 ± 0.65	43.36 ± 0.77
H_2O [% v/v]	12.70	10.83	15.84	13.93	9.67

The product gas after leaving the reactor passed through a set of two cyclones which were maintained at 400 ºC to prevent tars condensing. These cyclones separated the entrained particles from the gas stream, after which the gas passed through a hot filter (Candel element, Pyrotex BWF-Envirotec) kept at 450 ºC to remove the remaining smaller particles. The tar trap located after the hot filter was used to remove tars and water from the product gas. All the pipework upstream of the tar trap were heated and insulated. Finally, two parallel filters were used to avoid fine particles and tars passing to the gas analysis section.

When each experiment was finished, air and biomass were stopped as well as the electric furnaces and the whole system was cooled down to ambient temperature using an N_2 purge.

2.4. Sampling and analysis

The mass flow rate of product gas was measured before exiting the cleaning section using a Coriolis mass flow meter (Bronkhorst CORITECH). Product gas was sampled and analyzed online at 5 minute intervals using an Agilent Micro-GC 3000 equipped with a thermal conductivity detector for the determination of permanent gases and light hydrocarbons. For the determination of CO_2, C_2H_2, C_2H_4 and C_2H_6 a PLOT U column (30 μm/32 μm/ 8 m) was employed using helium as the carrier gas while a Molsieve (12 μm/320 μm/10 m) column using argon as the carrier gas was used to determine H_2, N_2, CH_4 and CO. Gas sampling started at the same time as biomass feeding and steady state conditions were achieved after 1.5 to 2 h (from when biomass feeding was started), and corresponded with the time needed to reach a constant temperature within the reactor. Gas composition was calculated as the mean gas composition during the steady state, when tar samples were also collected.

Tars were sampled using the Solid Phase Adsorption method (SPA) developed by Brage et al. [35] and later modified by Osipovs et al. [36]. 3 x 100 ml of gas and tars were taken over 2 min at 300 ºC using a programmable syringe pump (World Precision Instruments, Inc.) once the steady state was reached. The sampling point was located before the cold trap in order to avoid tar losses due to condensation (see Figure 1). After the experiment, the SPA samples were extracted with dichloromethane and analyzed by gas chromatography using two different instruments, an Agilent 7890A GC coupled to a triple-axis mass detector (MSD) 5975C was used for the identification of the tar compounds and a Thermo Scientific Trace 1310 GC equipped with a flame ionization detector (FID) for their quantification. In the GC-MSD helium was used as the carrier gas through a non-polar capillary column (HP-5MS, 30 m x 0.25 mm, 0.25 μm film thickness) at a constant flow rate of 1.2 ml/min. A sample volume of 0.8 μl was injected manually into an injection port maintained at 300 ºC in splitless mode. The oven temperature was initially 30 ºC for 5 minutes, then, heated to 180 ºC at 5 ºC/min, and finally to 300 ºC at 8 ºC/min. The MSD was configured to an ionization energy of 70 eV, full scan mode (50-550 m/z mass range), 2.91 scans/s with a solvent time delay of 1.95 min. The transfer line, MS source and MS quadrupole mass filter temperatures were kept at 300, 220 and 200 ºC respectively. The configuration of the GC-FID such as helium flow, type of capillary column, injection volume, injection port, and oven settings were kept the same as in the case of the GC-MSD. The FID temperature was 300 ºC and air, hydrogen and make up (N_2) flows were adjusted to 350, 35, and 40 ml/min respectively. 4-ethoxyphenol and tert-butylciclohexane were used as the internal standards for the GC-FID. Phenols were quantified using the 4-ethoxyphenol/phenol calibration curve and the remaining compounds with a tert-butylcyclohexane/naphthalene calibration curve. Chromeleon 7® was used to integrate the chromatograms in the range from benzene to benz[a]anthracene.

Tar results were calculated for normal conditions (NTP: 293.15 K and 101325 Pa). According to Siedlecki et al. [27] water vapour from the product gas condenses when passing through the sorbent, therefore, the sampled volume can be assumed to be taken on a dry basis (g/Nm^3 of raw

dry gas converted further to $g/kg_{biomass\text{-}daf}$). The results are reported as the mean value for several samples for each experiment, and they are presented as individual compounds as well as total GC detectable tar, secondary, and tertiary tar groups as defined by Milne et al. [5].

After each experiment, the bed material and char from the gasifier, particulates from the cyclones and hot filter, and water from the tar trap were discharged, weighed and kept for analysis. Cold gas efficiency (CGE) defined as the energy input over the potential energy output (eq. 1), and biomass conversion (eq. 2) were calculated to estimate the gasification performance. Carbon and hydrogen conversions were defined as the ratio of carbon or hydrogen mass flow in the dry product gas to the mass flow rate of the relevant element in the dry and ash free biomass. All the moisture from the product gas was assumed to be condensed out and collected in the tar trap. The mean moisture generation rate was calculated dividing the weight of water collected in the tar trap by the entire period of each gasification experiment, from the start of biomass feeding. Ultimate, moisture and ash content analyses were performed for all of these samples using a CHN-S elemental analyzer and a TGA respectively. The possible catalytic activity of the bed materials was analyzed using the enrichment factor of the elutriated fines defined according to Zevenhoven and Kilpinen [37] (eq. 3). Finally, a mass balance of the process was performed for each experiment. This calculation is useful for several reasons [7]: the input and output flows are compared checking the consistency of the results; unknown process flows and measurement errors can be determined; information regarding the gasification performance and efficiency is obtained and practical information can be collected to refine future experiments. Additionally, all this data is very important for the scale-up and design of the installation equipments for industrial facilities.

$$CGE = (LHV \cdot GY) / (m_{fuel} \cdot LHV_{fuel}) \cdot 100 \quad (1)$$

$$\text{Biomass conversion} = (1 - m_{char} / m_{fuel}) \cdot 100 \quad (2)$$

$$EF = [(\text{element concentration in fines})/(\text{element concentration in fuel})] \cdot [\%\text{ash in fuel}/100] \quad (3)$$

Two gasification experiments were performed with magnesite at 800 ºC, with the relative differences between replicates being smaller than 10 % which is in accordance with data reported by Siedlecki et al. [7].

3. Results and discussion

3.1. Effect of bed material and temperature on the product gas composition and gasification performance

The product gas composition is influenced by the operating temperature due to its effects on the chemical reactions during the gasification process. This parameter was varied using the electrical furnaces while the ER, the air flow rate and the biomass feeding rate were kept constant. The variation in gas composition as a function of temperature during the steady state operation is shown in Figure 2 for magnesite and olivine bed materials. In both cases, an increase in the H_2 and CO concentration was observed when temperature was increased. The concentration of CO_2 decreased with temperature while the concentration of light hydrocarbons remained almost constant. These effects can be explained by the chemical reactions which describe the gasification process [38]:

$$C + ½\ O_2 \rightarrow CO \qquad \Delta H = -111\ kJ/mol \tag{4}$$

$$CO + ½\ O_2 \rightarrow CO_2 \qquad \Delta H = -283\ kJ/mol \tag{5}$$

$$H_2 + ½\ O_2 \rightarrow H_2O \qquad \Delta H = -242\ kJ/mol \tag{6}$$

$$C + CO_2 \leftrightarrow 2\ CO \qquad \Delta H = +172\ kJ/mol \tag{7}$$

$$C + H_2O \leftrightarrow CO + H_2 \qquad \Delta H = +131\ kJ/mol \tag{8}$$

$$C + 2\ H_2 \leftrightarrow CH_4 \qquad \Delta H = -75\ kJ/mol \tag{9}$$

$$C_nH_m\ (tar) + nH_2O \rightarrow (n + m/2)\ H_2 + nCO \qquad \Delta H > 0 \tag{10}$$

$$C_nH_m\ (tar) + nCO_2 \rightarrow (m/2)\ H_2 + 2nCO \qquad \Delta H > 0 \tag{11}$$

As expected, higher temperatures favour products produced during endothermic reactions (eq. 7 and 8). The results showed the effect of the Boudouard (eq. 7) and water gas reactions (eq. 8) on the CO composition leading to a higher concentration with temperature. In the case of H_2, the water gas (eq. 8) favoured its production in spite of the methanation reaction (eq. 9). In addition, the higher concentration of H_2 and CO at higher temperature can be an indication of secondary tar reactions that convert primary tar into aromatics [39,40] and permanent gases, or tar cracking reactions such as steam reforming (eq. 10) enabled by the relatively high moisture content of cardoon (9.69 wt. %) and dry reforming (eq. 11) [41]. Overall the gas compositions for both magnesite and olivine were very similar for all gas species (Figure 2) with both bed materials having similar influences with increasing temperature. There were marginal differences in the H_2 content which was slightly lower for olivine than for magnesite while CO was slightly higher for olivine than for magnesite.

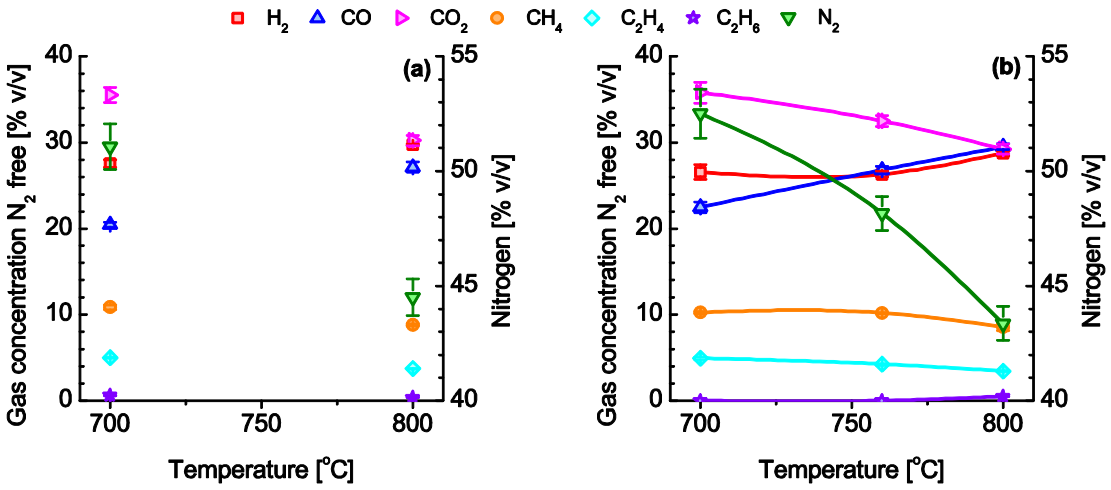

Figure 2. Gas composition (N_2 free) at different temperatures: a) magnesite and b) olivine.

The hydrogen content in the product gas was 12-16 %v/v (with N_2) for both magnesite and olivine which is relatively high for biomass gasification with air. Table 4 shows a brief comparison between the results obtained in this study and those reported in the literature for *C. cardunculus* gasification. Zabaniotou et al. [19] observed H_2 concentration of around 10 %v/v (with N_2) for fixed bed gasification of cardoon. While Christodoulou et al. [24] reported lower content of H_2, 8 %v/v (with N_2) for air gasification of a mixture of cardoon and giant reed using

olivine as the bed material. Similar observations were reported for air-steam gasification by Abelha et al. [23] who found higher concentration of H_2 for cardoon when compared to mixture of cardoon and eucalyptus. The differences in terms of H_2 content in the product gas between air gasification and air + steam/O_2 + steam gasification were relatively small, and cardoon was suggested by Zabaniotou et al. [19] to be a good feedstock for hydrogen production.

Table 4. Comparison of experimental results with the literature data (H_2 and CO calculated on an N_2 free basis).

Reference	System configuration	Operating conditions	H_2 (N_2 free) [% v/v]	CO (N_2 free) [% v/v]	Tar
Present study	Cardoon BFB, 13.45 cm of ID Bed material: magnesite	700-800 ºC ER: 0.2 Gasifying agent: air	28-30	20-27	29-27 (SPA) [g/Nm^3]
	Cardoon BFB, 13.45 cm of ID Bed material: olivine	700-800 ºC ER: 0.2 Gasifying agent: air	26-29	23-30	26-43 (SPA) [g/Nm^3]
Zabaniotou et al. [19]	Cardoon Fixed bed, 1.25 cm of ID	700-800 ºC ER: 0.2 Gasifying agent: air	28-11	20-38	31-38 wt. %
Christodoulou et al. [24]	Cardoon/giant reed (50/50%) CFB, 7.8 cm of ID Bed material: olivine	700-800 ºC ER: 0.3 Gasifying agent: air	22	29-35	6-3 (Tar protocol) [g/Nm^3]
	Cardoon CFB, 8.3 cm of ID Bed material: magnesite	700-750 ºC ER: 0.3 Gasifying agent: O_2+steam	35-37	7-8	134-122 (SPA) [g/Nm^3]
Encinar et al. [22]	Cardoon Fixed bed, 4 cm of ID	700-800 ºC Gasifying agent: steam (P_{H2O} = 0.53 atm)	59-60	17-19	NA
Abelha et al. [23]	Cardoon BFB, 8 cm of ID Bed material: silica sand	830 ºC ER: 0.1 Gasifying agent: air+steam	39	24	NA
	Cardoon/eucalyptus (50/50%) BFB, 8 cm of ID Bed material: silica sand+calcined olivine (15 wt. %)	830 ºC ER: 0.1 Gasifying agent: air+steam	37	21	4.1 (Tar protocol) [g/Nm^3]
	Cardoon/eucalyptus (50/50%) BFB, 8 cm of ID Bed material: silica sand+calcined dolomite (15wt. %)	830 ºC ER: 0.1 Gasifying agent: air+steam	38	20	NA

The hydrogen and carbon monoxide concentrations can be influenced by both the bed material and the biomass ash composition, particularly the content of alkali metals (potassium and sodium) [9], which are credited with improving gasification rate and yield of H_2 [42,43]. *C. cardunculus* has a high sodium and potassium contents (Table 1) which may account for the high production of H_2 obtained in the experiments. Higher molecular weight hydrocarbons may be reformed according to eq. 7 and eq. 8 to produce additional CO and H_2 using the surface of the catalyst/bed material [9].

The performance of the gasification experiments evaluated in terms of the gas yield (GY), lower heating value (LHV) of the gas as well as carbon and hydrogen conversion is shown in Figure 3. The data suggests that the GY, LHV of the product gas, carbon and hydrogen conversion as well as CGE increased with increasing gasification temperature for both bed materials. The carbon conversion seems to be influenced by the increased concentration of CO at higher temperatures in spite of the slight decrease in other carbon species such as CO_2, CH_4 and light hydrocarbons. The relatively low conversion of hydrogen when compared to carbon is mainly due to the hydrogen losses as water in the product gas, which condenses with the tar compounds as well as a lack of information regarding ammonia and hydrogen sulphide. The LHV increases with gasification temperature due to an increase in the concentration of the main combustible compounds, CO and H_2 in the product gas. GY increases slightly with temperature. This may be due to the greater gas production during the initial pyrolysis phase as well as the steam cracking and reforming of tars and the endothermic reactions of char gasification [44]. As a result of the rise in the LHV and the GY, the CGE also increased with temperature. Finally, biomass conversion showed a very high value, around 94%, when magnesite was used as the bed material. Magnesite appeared to exhibit a positive effect in terms char conversion particularly at lower temperature (700 ºC) since less char was collected from the gasifier after the test when compared to olivine (see appendix). Unlike magnesite, biomass conversion for olivine increased

with temperature which is consistent with the amount of char collected after gasification (see appendix).

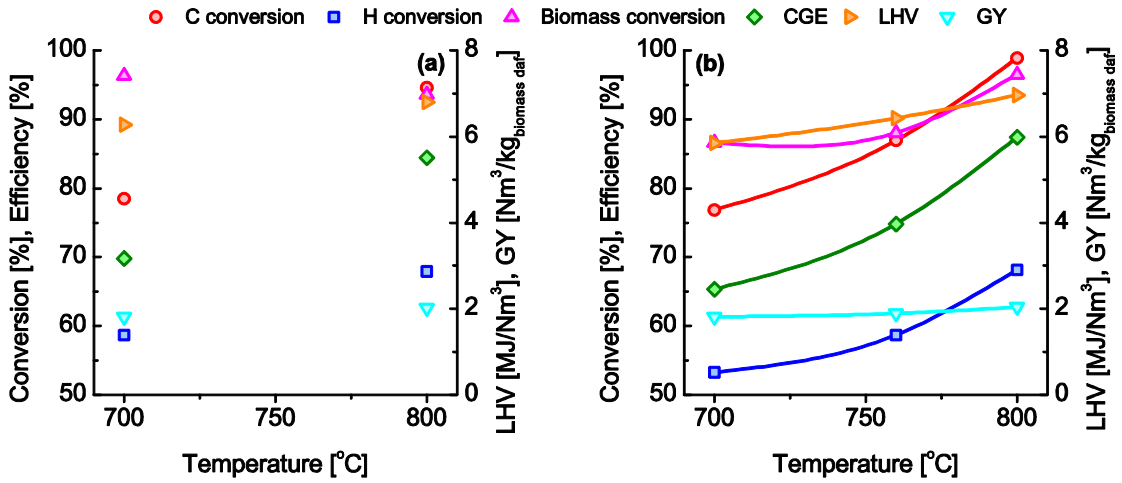

Figure 3. Gasification efficiency parameters: a) magnesite and b) olivine.

Some differences are apparent when comparing the gasification performance of the two bed materials, the data obtained showed some differences with temperature. Carbon and hydrogen conversion was slightly lower in the case of olivine at 700 ºC but a bit higher than magnesite at 800 ºC. Biomass conversion was much lower for olivine at 700 ºC. Similar results were obtained for the CGE and LHV of the product gas, with better performance observed with magnesite at low temperature and with olivine at high temperature. In terms of GY, the values were almost the same.

3.2. Effect of bed material and temperature on tar production

According to Milne et al. [5] tars can be classified into three different groups: primary, secondary and tertiary products. Primary tars are represented by cellulose-derived products. These type of tars released as low molecular weight oxygenated hydrocarbons are considered as completely converted into secondary tars at reactor temperatures above 600 ºC. Secondary tars are formed as phenols and substituted single ring aromatic species. Finally, tertiary tars are further divided into alkyl tertiary tars which are characterized as aromatics with substituent alkyl chains, and polyaromatic tertiary tars (PAH) without substituents. In this paper, the total

tar refers to total GC detectable tar including those tar compounds eluted from benzene (M ≈ 78.11 g/mol) to benz[a]anthracene (M ≈ 228.29 g/mol).

Figure 4 shows the influence of temperature and bed material on the distribution of tars using the above classification. In the case of magnesite (Figure 4a), the total tar decreased when temperature increased from 700 to 800 ºC, and a similar result was observed for secondary tars. Secondary tars consist of aromatic compounds with alkyl or hydroxyl substituent functional groups (see Table A2 in the appendix). With increasing temperature these functional groups are cleaved from the aromatic ring generating permanent gases CO, H_2, CO_2, CH_4, C_2H_4 and cyclopentadiene radicals, responsible for the increase of PAHs [45,46]. PAH tertiary tars (see Table A2) increased with temperature which is in accordance with observations reported in literature for magnesite in the same temperature range [47,48]. Increase of PAH tertiary tars could also be explained by the decomposition of the heavier GC undetectable fraction into lighter PAH tertiary tars [11]. The production of PAHs was observed together with a decrease in phenols and alkylated aromatics (Figure 5), as a result of dealkylation, dehydration, decarbonylation, and polymerization reactions [49,50]. The yield of alkyl tertiary tars (see Table A2) remained constant over the temperature range studied. The authors previous experimental observations as well as data from the scientific literature [51] indicates that alkyl tertiary tars decompose only above 800 ºC. However, the tertiary-alkyl tar group represented only 6.1 % of total tar at 800 ºC.

The trend for tar evolution using olivine as the bed material is presented in Figure 4b. An increase of total tar and secondary tars was observed between 700 to 750 ºC, followed by a decrease as the temperature rose to 800 ºC. The same trend was reported by other authors [5,48,52]. PAH tertiary tars increased with temperature and alkyl tertiary tars remained constant for the temperature range studied, which was also observed for magnesite. Comparison of magnesite and olivine does not indicate any difference in catalytic activity at 700 ºC. The yield of total tar at 700 ºC was slightly lower for olivine (26.3 g_{tar}/Nm^3) than for magnesite (28.9 g_{tar}/Nm^3). Delgado et al. [53,54] used magnesite in a secondary fixed bed catalytic reactor and

reported that at temperatures under 800 ºC the material was catalytically deactivated within 30 minutes, however, high tar conversion (more than 95%) was observed at temperatures above 850 ºC. Rapagnà et al. [14] and Devi et al. [11] also reported increased catalytic activity of olivine with temperature above 800 ºC. Regarding specific tar fractions, at 700 ºC the yield of secondary tars were similar for both magnesite and olivine, 15.7 and 16.4 g_{tar}/Nm^3, respectively. The same was observed when considering tertiary tars (alkyl and PAH tars) showing 5.7 g_{tar}/Nm^3 for magnesite and 4.2 g_{tar}/Nm^3 for olivine. A similar evolution profile to secondary and tertiary alkyl tars suggests that unknown tars mostly contain species from these two groups for olivine.

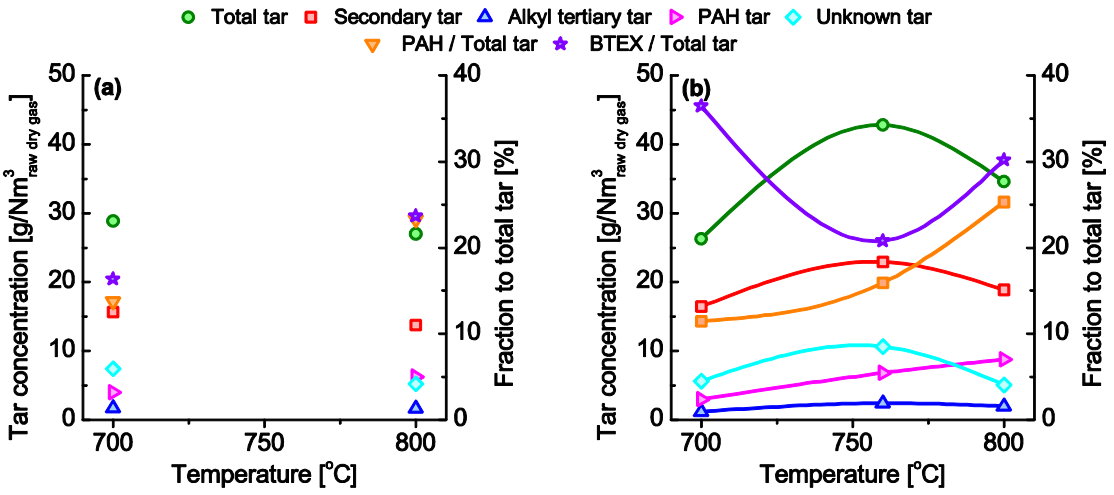

Figure 4. Tar concentration according Milne et al. classification [5]: a) magnesite and b) olivine.

In contrast, magnesite seemed to have slightly higher catalytic activity than olivine at 800 ºC. Total tar, secondary and tertiary tars were 27.0, 13.8 and 7.9 g_{tar}/Nm^3 for magnesite and, 34.6, 18.8 and 10.7 g_{tar}/Nm^3 for olivine. Hanping et al. [55] mixed magnesite and olivine with three types of biomasses prior to the feeding. They did not observe any significant difference in catalytic activity between the bed materials studied. Tar conversion rates varied only 4-5% between magnesite and olivine when total gravimetric tar was measured. Tar content in the product gas from the gasification of cardoon was measured by other researchers but comparison of results needs to be undertaken with caution due to the protocols employed for tar analysis, the units used for reporting, bed materials, gasifying agents etc Abelha et al. [23] (see Table 4 for

more details) analyzed tars according to tar protocol CEN/TS 15439. With silica sand, tar concentration was around of 7.5 g/Nm^3 while after addition of calcined olivine (15 % w/w) tar decreased to 4.1 g/Nm^3. Christodoulou et al. [24] reported total tar between 134.1 and 122.3 g/Nm^3 for cardoon using magnesite as the bed material and the tar protocol for tar analysis. On the other hand, a blend of 50 % w/w cardoon and 50 % w/w giant reed using olivine as the bed material and the SPA for tar analysis generated only between 5.9 and 2.8 g/Nm^3 of total tar. Rapagnà et al. [56] gasified crushed almond shells at 740 ºC using olivine and the tar protocol followed by HPLC/UV analysis. Total tar was 3.7 g/Nm^3 with toluene and naphthalene being the dominant tar species.

The 19 major tar compounds were identified and quantified and the results are presented in Figure 5 in the order in they were eluted. When magnesite was used as the bed material the dominant tar components were indane, o/m-cresol, toluene and naphthalene at both 700 and 800 ºC with naphthalene and toluene showing the highest concentration at 800 ºC. Whereas, for olivine benzene, toluene and indane were the dominant compounds at 700 ºC, with toluene, naphthalene and benzene at 800 ºC. The BTEX (benzene, toluene, ethylbenzene and xylene) fraction in total tar was higher for olivine when compared to magnesite, increasing in the case of magnesite and showing a decrease between 700 and 760 ºC and an increase from 760 to 800 ºC for olivine. The yield of naphthalene was the highest among PAH tar species and all PAHs increased with the process temperature. Fraction of PAHs in the total tar increased with increasing temperature, from 11 to 15 % for olivine and from 14 to 23 % for magnesite. Although total tar decreased with temperature, the increase in polyaromatic compounds (naphthalene, acenaphthylene, anthracene, pyrene) gives rise to a higher tar dew point which is an important parameter in predicting tar condensation in the downstream devices. Phenolic tar species were significant only at or below 750 ºC, however, at 800 ºC oxygen containing species drastically decreased. Nevertheless, phenols and cresols are water soluble making them easier to remove using water scrubbers. In general, the observed trends for tars with respect to temperature are in agreement with previous studies for other biomasses [24,40]. The evolution

of individual tar compounds with gasification temperature indicates that catalytic processes such as dealkylation, decarbonylation, dehydrogenation, and dehydration reactions of substituted tar species become more significant above 760 ºC.

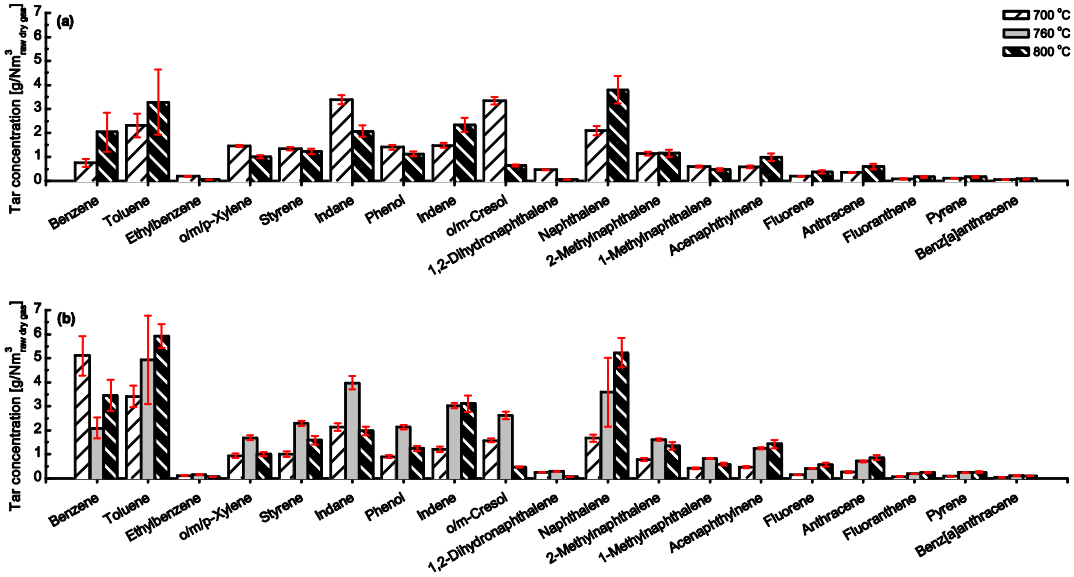

Figure 5. Tar concentration for individual compounds: a) magnesite and b) olivine.

Arena et al. [57] reported that olivine is an effective in situ tar reduction agent when plastic waste is gasified. The iron and magnesium contained in the olivine can activate the endothermic tar decomposition reactions [58]. Iron catalytically enhances dehydrogenation and carbon formation reactions (eq. 12):

$$C_nH_m \rightarrow n\ C + (m/2)\ H_2 \quad (12)$$

while, the magnesium oxide promotes the cracking and isomerization reactions of the hydrocarbon fragments produced by thermal cracking of the feedstock (eq. 13):

$$p\ C_xH_y \rightarrow q\ C_nH_m + r\ H_2 \quad (13)$$

All the series/parallel reactions of cracking, isomerisation, hydro-cyclization, aromatization, oligomerization, polymerization produce coke and molecular hydrogen (H_2).

In order to investigate the catalytic activity of olivine and magnesite, the inorganic fraction of elutriated fines collected in the cyclones and hot filter were analysed and the results for cyclone 1 are presented in Table 5. Table 5 also reports the ratio between the mass flow rate of each element that escapes from the gasifier as fines and that which remains in the reactor as the inorganic fraction of the fuel ($Q_{i,fines}/Q_{i,fuel}$), as well as the enrichment factor EF in the elutriated fines.

Table 5. Composition of inorganic fraction and enrichment factor (EF) of fines collected in cyclone 1 for gasification temperature of 800 ºC.

	Magnesite 800 ºC			**Olivine 800 ºC**		
	mg/kg $_{elutriated\ fines,\ db}$	$Q_{i,fines}/Q_{i,fuel}$	EF	mg/kg $_{elutriated\ fines,\ db}$	$Q_{i,fines}/Q_{i,fuel}$	EF
Aluminium	73664.0	0.29	0.61	69928.4	0.22	0.58
Cadmium	26.3	0.06	0.12	26.5	0.05	0.12
Calcium	44319.8	0.13	0.27	71459.7	0.17	0.43
Cobalt	36.4	0.07	0.15	37.8	0.06	0.16
Copper	789.2	0.07	0.14	816.7	0.06	0.15
Chromium	424.9	1.84	3.85	826.9	2.92	7.50
Iron	7386.6	0.34	0.72	10718.9	0.41	1.05
Magnesium	84895.7	2.04	4.28	32565.2	0.64	1.64
Manganese	280.1	0.24	0.50	334.6	0.23	0.60
Molybdenum	151.8	0.08	0.17	122.5	0.05	0.14
Nickel	542.1	0.57	1.20	599.6	0.52	1.32
Lead	29.3	1.27	2.66	84.7	3.00	7.68
Potassium	52920.7	0.27	0.56	61353.2	0.25	0.65
Selenium	617.2	0.05	0.10	530.8	0.03	0.09
Sodium	52414.7	0.09	0.19	49715.5	0.07	0.18
Silicon	190028.8	0.24	0.50	187836.9	0.19	0.50
Zinc	78.9	0.11	0.23	93.9	0.11	0.27

According to Arena et al. [58], when olivine provides a significant catalytic activityfor tar cracking and carbonization, the fines collected in the cyclone contain substantially larger quantities of iron than those remaining in the reactor with fuel; consequently they observed values of $Q_{Fe,\ fines}/Q_{Fe,\ fuel}$ significantly larger than 1, typically 100 or more. The results presented in Table 5 for the gasification of cardoon suggest that $Q_{Fe,\ fines}/Q_{Fe,\ fuel}$ is 0.34 for magnesite and 0.41 for olivine and it is increasing with temperature (data not presented). This implies that the catalytic activity of olivine is absent, or only partially present during air gasification of cardoon. The values of the enrichment factor EF in the collected fines are larger

than 1 for olivine and below 1 for magnesite suggesting that the ash enrichment in iron is influenced by the composition of the olivine particles.

Similar results were reported by Arena and Di Gregorio [59] for the gasification of solid recovered fuel. They concluded that magnesium was active for the cracking and isomerisation reactions, but the dehydrogenation and carbonization reactions which required active sites of elemental iron were absent, and tar formation was not inhibited. The explanation provided by Arena and Di Gregorio [59] may also be valid for the gasification of cardoon i.e. with the high ash and Fe content in cardoon, the metals in the ash can act as competing active sites to the iron oxides on the external surface of olivine particles so avoiding their reduction to elemental Fe. On the other hand, fully oxidized iron phases containing Fe^{3+} ions in the presence of potassium are known to be highly catalytically active towards dehydrogenation of ethylbenzene to styrene generating H_2 [60]. The content of ehtylbenzene in the tar was relatively low while styrene was high (Figure 5) suggesting that dehydrogenation of substituted aromatic hydrocarbons with long aliphatic chains is a possible explanation for a high hydrogen content in the product gas.

Moreover, the magnesium was catalytically active particularly in magnesite (EF = 4.28) but also in olivine (EF = 1.64) possibly enhancing the dehydrogenation and isomerisation reactions of fragments produced by thermal cracking of biomass [61]. Rabou et al. [47] reported that Mg present in chicken manure ash was very active in cracking of 4 and 5-ring tar compounds even at 750°C.

Comparison of bed materials indicates that there is no significant difference in terms of the yield of total tar between magnesite and olivine but the composition of tar is very different. The BTEX fraction in the measured total tar was higher for olivine when compared to magnesite while the PAH fraction in the total tar was similar for both bed materials. Magnesite seems to be more catalytically active at 800 ºC than olivine

3.3. Mass balance

The consistency of the results was evaluated by performing a mass balance for the different main elements based on the total flows, on a dry-ash free basis. The results are presented for experiments with magnesite and olivine at 800 ºC (Table 6). The biomass input was differentiated into dry-ash free biomass, moisture and ash. The elemental flow rate of biomass was calculated according to the elemental and proximate analysis shown in Table 1. The other input flows were the air for fluidization and the N_2 used to pressurize the hopper. The mass output flows were segregated into product gas, char and ash accumulated in the bed, cyclones and hot filter, and total moisture from the char particles and moisture collected from the tar trap, and tar. This last stream was the total GC detectable tar obtained using the SPA method.

Table 6. Mass balance for the cases of magnesite and olivine at 800 ºC.

Magnesite 800 ºC						
	Mass flow	C	H	N	O	Ash [g db/h]
Biomass [kg daf/h]	3.56	1.57	0.23	0.02	1.74	456.44
Biomass moisture [g/h]	430.66		47.85		382.81	
Air [kg/h]	4.53			3.46	1.06	
N_2 for feeding [kg/h]	0.14			0.14		
Total input [kg/h]	**9.11**	**1.57**	**0.28**	**3.62**	**3.18**	**456.44**
Gas [kg/h]	7.73	1.49	0.19	3.72	2.33	
Char gasifier [g daf/h]	152.51	81.39	1.27	0.69	69.16	114.66
Char cyclone 1 [g daf/h]	55.37	14.09	0.22	0.12	40.94	158.84
Char cyclone 2 [g daf/h]	3.90	0.88	0.01	0.01	3.00	13.20
Char filter [g daf/h]	15.19	3.70	0.03	0.03	11.43	46.58
Total moisture [g/h]	704.50		78.20		626.30	
Tar (all as naphthal.) [g/h]	194.50	182.27	12.24			
Total output [kg/h]	**9.19**	**1.77**	**0.28**	**3.72**	**3.08**	**333.28**
Out/In [%]	100.87	112.58	101.27	102.83	96.82	73.02
Olivine 800 ºC						
	Mass flow	C	H	N	O	Ash [g db/h]
Biomass [kg daf/h]	3.51	1.55	0.23	0.02	1.72	451.06
Biomass moisture [g/h]	425.58		47.29		378.30	
Air [kg/h]	4.50			3.44	1.06	
N2 for feeding [kg/h]	0.14			0.14		
Total input [kg/h]	**9.03**	**1.55**	**0.27**	**3.60**	**3.15**	**451.06**
Gas [kg/h]	7.74	1.54	0.19	3.63	2.39	
Char gasifier [g daf/h]	79.94	33.38	0.95	0.50	45.11	80.26
Char cyclone 1 [g daf/h]	36.67	6.65	0.17	0.11	29.74	136.33
Char cyclone 2 [g daf/h]	2.80	0.37	0.01	0.01	2.41	14.78
Char filter [g daf/h]	4.40	0.62	0.01	0.02	3.75	22.28
Total moisture [g/h]	621.80		69.10		552.70	

Tar (all as naphthal.) [g/h]	249.84	234.13	15.72			
Total output [kg/h]	**8.99**	**1.81**	**0.27**	**3.63**	**3.03**	**253.64**
Out/In [%]	99.56	116.62	99.66	100.76	95.97	56.23

The mass balance, either the total mass flow or elemental species, showed more than 88% agreement between input and output. The highest difference was observed in the C balance which is explained due to the assumption of considering all tar as naphthalene. There were also some differences in the O and H balance that could be due to the lack of information about hydrogen rich component such as ammonia, hydrogen sulphide and acetylene as well as the accuracy of water content determination. The nitrogen balance was closed to 100% as was expected due to the inert properties of this species. It is worth noticing that the ash balance showed large differences between output and input values, around 73% for magnesite and 56% for olivine. This discrepancy was attributed to ash accumulation in the horizontal pipes and hot filter.

Figure 6 shows the generation of the different residual output flows: char, ash, moisture and GC detectable tar. Tar, char and ash generation rates were low in the experiments with magnesite (< 0.1 $kg/kg_{biomass\ daf}$) for the two temperatures tested. Moisture generation was also relatively low, around 0.2 $kg/kg_{biomass\ daf}$. Char and ash generation increased with temperature while moisture decreased. This indicates that magnesite may be more effective towards char reactivity at low temperature. On the other hand, when olivine particles were used, char and moisture generation were higher at 700 ºC and decreased sharply at 800 ºC, this could be an indicator of improved char reactivity at higher temperature due to the catalytic properties of olivine or some ash components (potassium and sodium) as well as significantly improved, water gas shift reaction ($CO + H_2O \leftrightarrow CO_2 + H_2$) or steam tar reforming (eq. 10). The mass balance showed higher ash deposition in pipes and other elements of the facility at lower temperatures for olivine and at higher temperature for magnesite. Temperature should not have a significant effect on the ash quantity collected downstream of the gasifier and the differences in the ash collected could be due to permanent accumulation of the ash in the hot filter element. In general terms, magnesite

showed less char and moisture at low temperature, while olivine produced lower char, ash and moisture at the higher temperature.

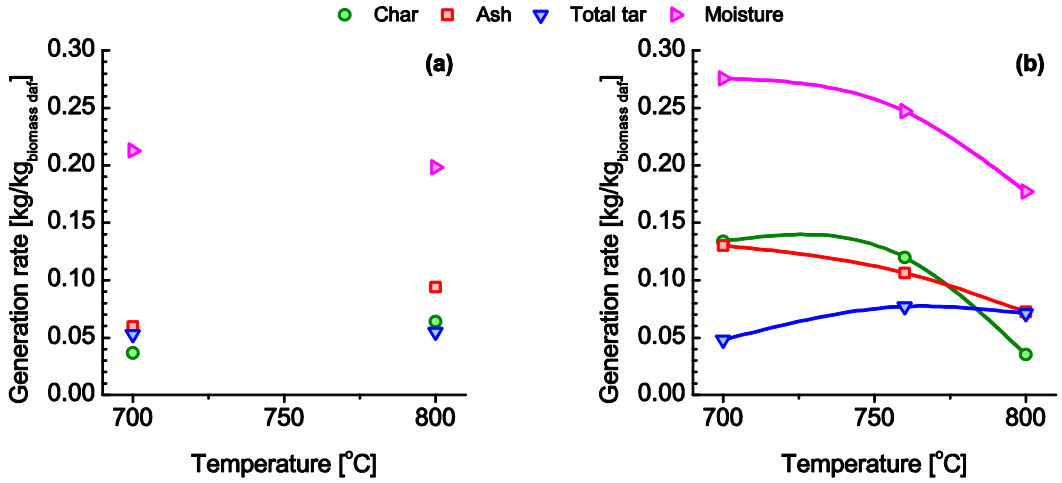

Figure 6. Char, ash, moisture and total GC detectable tar per kilogram of dry-ash free of biomass: a) magnesite and b) olivine.

Figure 7 shows a flow diagram describing the mass balance for carbon for experiments at 800 ºC. Carbon losses due to elutriated particles were very small compared with the carbon introduced into the reactor. In the case of magnesite, higher amounts of carbon were found in the cyclones and hot filter than in the case of olivine. The carbon accumulated in the bed was also higher with magnesite than with olivine indicating a higher gasification rate when olivine was used as a bed material. As stated above, the carbon balance shows gaps in the mass closure as a consequence of considering all tar as naphthalene. Thus the values in Figure 7 do not fit well.

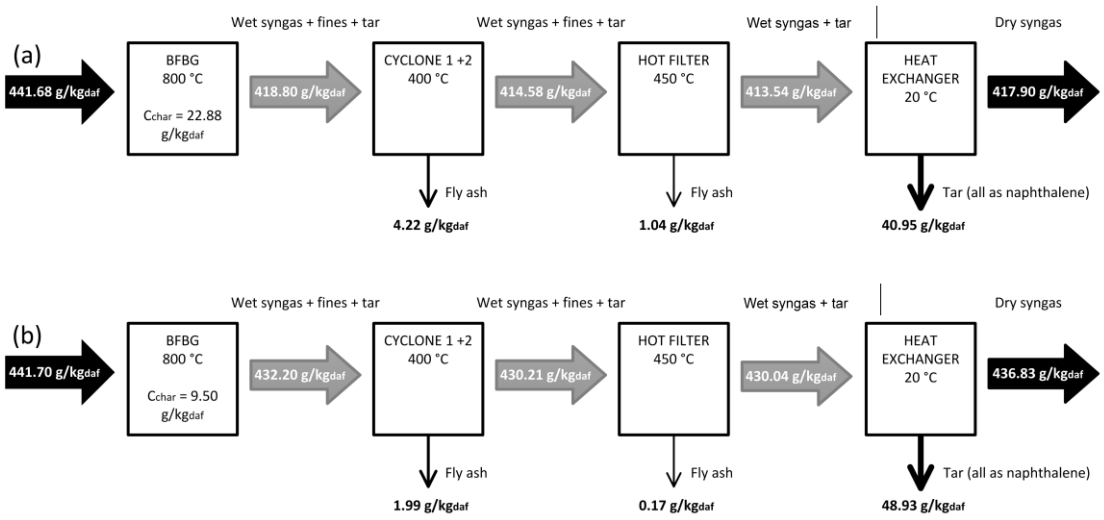

Figure 7. Carbon balance diagram for gasification at 800 ºC: a) magnesite and b) olivine.

4. Conclusions

C. cardunculus L. was gasified in a pilot scale BFB reactor at different temperatures using bed materials while maintaining both the ER and fluidization regime constant.

Relatively high hydrogen content in the product gas was obtained for both magnesite and olivine. The use of magnesite and olivine as well as the high alkali metals present in cardoon ashes contributed to achieving the high concentration of hydrogen observed, by acting as catalytic agents. The product gas quality in terms of LHV and gas yield was improved with increasing temperature. Greater than 90% carbon and biomass conversions were achieved at the highest temperature tested (800 ºC) for the two bed materials. For the gasification experiments carried out at 800 ºC the amount of chemical energy of cardoon transferred into the product gas were 84% and 87% for magnesite and olivine respectively.

The addition of kaolin to the biomass prevented agglomeration in spite of the well known sintering behaviour of *C. cardunculus* L. ashes suggesting that it could be used for gasifying high alkali content biomass, mitigating the problems for long term operation.

Not significant difference in terms of the yield of total tar between magnesite and olivine was observed, however, the composition of tar is very different. The BTEX fraction in the measured

total tar was higher for olivine when compared to magnesite while the PAH fraction in the total tar was similar for both bed materials. Magnesite seems to be more catalytically active at 800 ºC than olivine.

The catalytic activity due to the iron in the olivine was very small during cardoon air gasification at 800 ºC. However, magnesium in the magnesite and to a lesser extent in the olivine exhibited catalytic active behaviour towards tar cracking.

In general terms, magnesite provided better gasification performance at lower temperatures (700 ºC) (gas composition, biomass conversion, LHV, gas yield and char conversion) than olivine while olivine performed better at high temperature (800 ºC). Tar concentration remained high in the product gas application so additional downstream gas cleaning would be necessary for both magnesite and olivine. The results suggest that the best option is to use olivine at 800 ºC for *C. cardunculus* gasification or if agglomeration could be avoided by use of kaolin temperature in excess of this could further reduce the tar content.

Abbreviations

BFB	bubbling fluidized bed
BTEX	benzene, toluene, ethylbenzene and xylene
CGE	cold gas efficiency
ER	equivalent ratio
FID	flame ionization detector
GC	gas chromatography
GY	gas yield
HHV	high heating value
ICP	inductive coupled plasma

ID	inner diameter
LHV	low heating value
MSD	mass spectrum detector
NTP	normal temperature and pressure conditions
PAH	polyaromatic hydrocarbons
SPA	solid phase adsorption
TGA	thermogravimetric analyzer

Acknowledgements

The authors would like to express their gratitude to the financial support of the Spanish Ministry of Economy and Competiveness from project ENE2014-54942-R. The financial support provided by Enterprise Ireland Competence Centre for Biorefining & Biofuels (CC/2009/1305A) and INTERREG IVB NEW REsource Innovation Network for European Waste Project number 317J-RENEW as research grants are gratefully acknowledged.

References

[1] P. Basu, Biomass Gasification and Pyrolysis: Practical Design and Theory, Elsevier Inc., Amsterdam, 2010.

[2] A. Klein, Gasification: an alternative process for energy recovery and disposal of municipal solid wastes, M.S. Thesis in Earth Resources Engineering. Columbia University, New York, 2002.

[3] D. Kunii, O. Levenspiel, Fluidization engineering, 2nd ed., Butterworth-Heinemann, 1991.

[4] R. Warnecke, Gasification of biomass: comparison of fixed bed and fluidized bed gasifier, Biomass and Bioenergy. 18 (2000) 489–497.

[5] T.A. Milne, R.J. Evans, N. Abatzoglou, Biomass Gasifier " Tars ": Their Nature ,

Formation and Conversion, 1998.

[6] J.H.A. Kiel, S.V.B. van Paasen, J.P.A. Neeft, L. Devi, K.J. Ptasinski, F.J.J.G. Janssen, et al., Primary measures to reduce tar formation in fluidised-bed biomass gasifiers, 2004.

[7] M. Siedlecki, R. Nieuwstraten, E. Simeone, W. de Jong, A.H.M. Verkooijen, Effect of magnesite as bed material in a 100 kWth steam-oxygen blown circulating fluidized-bed biomass gasifier on gas composition and tar formation, Energy & Fuels. 23 (2009) 5643–5654.

[8] J. Werther, M. Saenger, E.-U. Hartge, T. Ogada, Z. Siagi, Combustion of agricultural residues, Prog. Energy Combust. Sci. 26 (2000) 1–27.

[9] D. Sutton, B. Kelleher, J.R.H. Ross, Review of literature on catalysts for biomass gasification, Fuel Process. Technol. 73 (2001) 155–173.

[10] J. Corella, J.M. Toledo, R. Padilla, Olivine or Dolomite as In-Bed Additive in Biomass Gasification with Air in a Fluidized Bed : Which Is Better?, Energy & Fuels. 18 (2004) 713–720.

[11] L. Devi, K.J. Ptasinski, F.J.J.G. Janssen, S.V.B. van Paasen, P.C.A. Bergman, J.H.A. Kiel, Catalytic decomposition of biomass tars: use of dolomite and untreated olivine, Renew. Energy. 30 (2005) 565–587.

[12] F. Miccio, B. Piriou, G. Ruoppolo, R. Chirone, Biomass gasification in a catalytic fluidized reactor with beds of different materials, Chem. Eng. J. 154 (2009) 369–374.

[13] M.L. Mastellone, U. Arena, Olivine as a tar removal catalyst during fluidized bed gasification of plastic waste, AIChE J. 54 (2008) 1656–1667.

[14] S. Rapagnà, N. Jand, a. Kiennemann, P.U. Foscolo, Steam-gasification of biomass in a fluidised-bed of olivine particles, Biomass and Bioenergy. 19 (2000) 187–197.

[15] J. Corella, J.M. Toledo, G. Molina, Biomass gasification with pure steam in fluidised bed: 12 variables that affect the effectiveness of the biomass gasifier, Int. J. Oil, Gas Coal Technol. 1 (2008) 194.

[16] R. Zwart, S. Van Der Heijden, R. Emmen, J.D. Bentzen, P. Stoholm, J. Krogh, Tar removal from low-temperature gasifiers. ECN-C-10-008, 2010.

[17] P. Grammelis, A. Malliopoulou, P. Basinas, N.G. Danalatos, Cultivation and characterization of Cynara Cardunculus for solid biofuels production in the Mediterranean region, Int. J. Mol. Sci. 9 (2008) 1241–58.

[18] J. Fernández, M.D. Curt, State of the art of Cynara Cardunculus L. as an energy crop,

in: L. Sjunnesson, J.E. Carrasco, P. Helm, A. Grassi (Eds.), 14th Eur. Conf. Technol. Exhib. Biomass Energy, Ind. Clim. Prot., ETA-Renewable Energies and WIP Renewable Energies, Paris, 2005: pp. 22–27.

[19] A. Zabaniotou, P. Bitou, T. Kanellis, P. Manara, G. Stavropoulos, Investigating Cynara C . biomass gasification producer gas suitability for CHP, second generation biofuels, and H2 production, Ind. Crop. Prod. 61 (2014) 308–316.

[20] J.M. Encinar, J.F. González, J. González, Fixed-bed pyrolysis of Cynara cardunculus L . Product yields and compositions, Fuel. 68 (2000) 209–222.

[21] J. Herguido, J. Corella, J. González-Saiz, Steam Gasification of Lignocellulosic Residues in a Fluidized Bed at a Small Pilot Scale . Effect of the Type of Feedstock, Ind. Eng. Chem. Res. 31 (1992) 1274–1282.

[22] J.M. Encinar, J.F. González, J. González, Steam gasification of Cynara cardunculus L .: influence of variables, Fuel Process. Technol. 75 (2002) 27–43.

[23] P. Abelha, C. Franco, F. Pinto, H. Lopes, I. Gulyurtlu, J. Gominho, et al., Thermal Conversion of Cynara cardunculus L . and Mixtures with Eucalyptus globulus by Fluidized-Bed Combustion and Gasification, Energy & Fuels. 27 (2013) 6725–6737.

[24] C. Christodoulou, C. Tsekos, G. Tsalidis, M. Fantini, K.D. Panopoulos, W. de Jong, et al., Attempts on cardoon gasification in two different Circulating fluidized Beds, Case Stud. Therm. Eng. 4 (2014) 42–52.

[25] C. Christodoulou, E.-I. Koytsoumpa, K.D. Panopoulos, S. Karellas, E. Kakaras, Agglomeration problems during cardoon fluidized bed gasification, Therm. Sci. 18 (2014) 645–656.

[26] D. Serrano, S. Sánchez-Delgado, C. Sobrino, C. Marugán-Cruz, Defluidization and agglomeration of a fluidized bed reactor during Cynara cardunculus L. gasification using sepiolite as a bed material, Fuel Process. Technol. 131 (2015) 338–347.

[27] M. Siedlecki, W. de Jong, Biomass gasification as the first hot step in clean syngas production process – gas quality optimization and primary tar reduction measures in a 100 kW thermal input steam–oxygen blown CFB gasifier, Biomass and Bioenergy. 35 (2011) S40–S62.

[28] B.-M. Steenari, O. Lindqvist, High-temperature reactions of straw ash and the anti-sintering additives kaolin and dolomite, Biomass and Bioenergy. 14 (1998) 67–76.

[29] M.J. Fernández, P.D. Arocas, L.G. Nebot, J.E.C. García, The effect of the addition of chemical materials on the sintering of biomass ash, Fuel. 87 (2008) 2651–2658.

[30] K. Weber, P. Quicker, Enhancing ash melting behaviour of straw ash through the

addition of kaolin, in: 21st Eur. Biomass Conf. Exhib., Copenhagen, 2013: pp. 1447–1450.

[31] G. Xue, M. Kwapinska, W. Kwapinski, K.M. Czajka, J. Kennedy, J.J. Leahy, Impact of torrefaction on properties of Miscanthus × giganteus relevant to gasification, Fuel. 121 (2014) 189–197.

[32] S. Fournel, J.H. Palacios, R. Morissette, J. Villeneuve, S. Godbout, M. Heitz, et al., Influence of biomass properties on technical and environmental performance of a multi-fuel boiler during on-farm combustion of energy crops, Appl. Energy. 141 (2015) 247–259.

[33] D. Geldart, Types of Gas Fluidization, Powder. 7 (1973) 285–292.

[34] G. Xue, M. Kwapinska, A. Horvat, Z. Li, S. Dooley, W. Kwapinski, et al., Gasification of Miscanthus x giganteus in an Air-Blown Bubbling Fluidized Bed: A Preliminary Study of Performance and Agglomeration, Energy & Fuels. 28 (2014) 1121–1131.

[35] C. Brage, Q. Yu, G. Chen, K. Sjöström, Use of amino phase adsorbent for biomass tar sampling and separation, Fuel. 76 (1997) 137–142.

[36] S. Osipovs, Comparison of efficiency of two methods for tar sampling in the syngas, Fuel. 103 (2013) 387–392.

[37] R. Zevenhoven, P. Kilpinen, Control of Pollutants in Flue Gases and Fuel Gases, 3rd ed., Helsinki University of Technology Espoo, Espoo/Turku, 2004.

[38] C. Higman, M. van der Burgt, Gasification, 1st ed., Gulf Professional Publishing, Amsterdam, 2003.

[39] M.L. Boroson, J.B. Howard, J.P. Longwell, W. a. Peters, Heterogeneous cracking of wood pyrolysis tars over fresh wood char surfaces, Energy & Fuels. 3 (1989) 735–740.

[40] P. Morf, P. Hasler, T. Nussbaumer, Mechanisms and kinetics of homogeneous secondary reactions of tar from continuous pyrolysis of wood chips, Fuel. 81 (2002) 843–853.

[41] P. Lahijani, Z.A. Zainal, Gasification of palm empty fruit bunch in a bubbling fluidized bed: A performance and agglomeration study, Bioresour. Technol. 102 (2011) 2068–2076.

[42] R.C. Brown, Q. Liu, G. Norton, Catalytic effects observed during the co-gasification of coal and switchgrass, Biomass and Bioenergy. 18 (2000) 499–506.

[43] A. Demirbaş, Gaseous products from biomass by pyrolysis and gasification: Effects of

catalyst on hydrogen yield, Energy Convers. Manag. 43 (2002) 897–909.

[44] F. Pinto, C. Franco, R.N. André, C. Tavares, M. Dias, I. Gulyurtlu, et al., Effect of experimental conditions on co-gasification of coal, biomass and plastics wastes with air/steam mixtures in a fluidized bed system, Fuel. 82 (2003) 1967–1976.

[45] E.M. Fitzpatrick, J.M. Jones, M. Pourkashanian, A.B. Ross, A. Williams, K.D. Bartle, Mechanistic Aspects of Soot Formation from the Combustion of Pine Wood, Energy & Fuels. 22 (2008) 3771–3778.

[46] H. Yu, Z. Zhang, Z. Li, D. Chen, Characteristics of tar formation during cellulose, hemicellulose and lignin gasification, Fuel. 118 (2014) 250–256.

[47] L.P.L.M. Rabou, R.W.R. Zwart, B.J. Vreugdenhil, L. Bos, Tar in biomass producer gas, the Energy research Centre of The Netherlands (ECN) experience: An enduring challenge, Energy and Fuels. 23 (2009) 6189–6198.

[48] C.M. Kinoshita, Y. Wang, J. Zhou, Tar formation under different biomass gasification conditions, J. Anal. Appl. Pyrolysis. 29 (1994) 169–181.

[49] Q. Yu, C. Brage, G. Chen, K. Sjöström, Temperature impact on the formation of tar from biomass pyrolysis in a free-fall reactor, J. Anal. Appl. Pyrolysis. 40-41 (1997) 481–489.

[50] C. Berrueco, D. Montané, B. Matas Güell, G. del Alamo, Effect of temperature and dolomite on tar formation during gasification of torrefied biomass in a pressurized fluidized bed, Energy. 66 (2014) 849–859.

[51] A. Dufour, E. Masson, P. Girods, Y. Rogaume, A. Zoulalian, Evolution of aromatic tar composition in relation to methane and ethylene from biomass pyrolysis-gasification, Energy and Fuels. 25 (2011) 4182–4189.

[52] S.V.B. van Paasen, J.H.A. Kiel, Tar formation in a fluidised-bed gasifier: Impact of fuel properties and operating conditions. ECN-C-04-013, 2004.

[53] J. Delgado, M.P. Aznar, J. Corella, Calcined dolomite, magnesite, and calcite for cleaning hot gas from a fluidized bed biomass gasifier with steam: life and usefulness, Ind. Eng. Chem. Res. 35 (1996) 3637–3643.

[54] J. Delgado, M.P. Aznar, J. Corella, Biomass gasification with steam in fluidized bed: effectiveness of CaO, MgO, and CaO-MgO for hot raw gas cleaning, Ind. Eng. Chem. Res. 36 (1997) 1535–1543.

[55] C. Hanping, L. Bin, Y. Haiping, Y. Guolai, Z. Shihong, Experimental investigation of biomass gasification in a fluidized bed reactor, Energy & Fuels. 22 (2008) 3493–3498.

[56] S. Rapagnà, K. Gallucci, M. di Marcello, M. Matt, M. Nacken, S. Heidenreich, et al., Gas cleaning, gas conditioning and tar abatement by means of a catalytic filter candle in a biomass fluidized-bed gasifier, Bioresour. Technol. 101 (2010) 7123–7130.

[57] U. Arena, L. Zaccariello, M.L. Mastellone, Tar removal during the fluidized bed gasification of plastic waste, Waste Manag. 29 (2009) 783–791.

[58] U. Arena, L. Zaccariello, M.L. Mastellone, Fluidized bed gasification of waste-derived fuels, Waste Manag. 30 (2010) 1212–1219.

[59] U. Arena, F. Di Gregorio, Gasification of a solid recovered fuel in a pilot scale fluidized bed reactor, Fuel. 117 (2014) 528–536.

[60] X.M. Zhu, M. Schön, U. Bartmann, a. C. Van Veen, M. Muhler, The dehydrogenation of ethylbenzene to styrene over a potassium-promoted iron oxide-based catalyst: A transient kinetic study, Appl. Catal. A Gen. 266 (2004) 99–108.

[61] L. Di Felice, C. Courson, D. Niznansky, P.U. Foscolo, A. Kiennemann, Biomass gasification with catalytic tar reforming: A model study into activity enhancement of calcium- and magnesium-oxide-based catalytic materials by incorporation of iron, Energy and Fuels. 24 (2010) 4034–4045.

Appendix

Table A1. Operating conditions and results from each gasification experiment.

Operating conditions					
Bed material	magnesite	magnesite	olivine	olivine	olivine
Bed material loaded [kg]	5.70	5.70	5.38	5.38	5.38
Biomass feeding rate [kg_{daf}/h]	3.63	3.56	3.51	3.60	3.52
Biomass throughput daf [kg_{daf}/m^2h]	255.55	250.37	247.17	253.53	247.42
Air flow rate [Ndm^3/min]	63.43	63.47	62.79	63.36	63.13
ER [–]	0.20	0.20	0.20	0.20	0.20
u/u_{mf} [–]	2.91	3.06	3.01	3.19	3.35
Inlet air temperature, TIC02 [ºC]	209	270	227	276	320
Gasifcation temperature, TIC10 [ºC]	700	800	700	760	800
TIC06 [ºC]	701	756	718	741	791
Syngas composition (dry) and process results					
H_2 [% v/v]	13.48 ± 0.38	16.51 ± 0.27	12.62 ± 0.82	13.64 ± 0.36	16.26 ± 0.33
CO [% v/v]	10.01 ± 0.23	15.05 ± 0.52	10.68 ± 0.66	13.89 ± 0.40	16.71 ± 0.30
CH_4 [% v/v]	5.33 ± 0.18	4.89 ± 0.10	4.88 ± 0.06	5.29 ± 0.09	4.87 ± 0.26
CO_2 [% v/v]	17.37 ± 0.17	16.77 ± 0.07	16.98 ± 0.18	16.83 ± 0.08	16.56 ± 0.12
C_2H_4 [% v/v]	2.45 ± 0.03	2.07± 0.01	2.34 ± 0.02	2.19 ± 0.03	1.96 ± 0.03
C_2H_6 [% v/v]	0.30 ± 0.01	0.22 ± 0.00	0.00 ± 0.00	0.00 ± 0.00	0.29 ± 0.01
N_2 [% v/v]	51.07 ± 1.18	44.50 ± 0.71	52.51 ± 1.11	48.16 ± 0.65	43.36 ± 0.77
H_2O [% v/v]	12.70	10.83	15.84	13.93	9.67
Low heating value [MJ/Nm^3]	6.28	6.80	5.85	6.42	6.96
Gas yield [$Nm^3/kg_{biomass\ daf}$]	1.81	2.02	1.82	1.90	2.04
Carbon conversion [%]	78.52	94.62	76.82	86.92	98.90
Hydrogen conversion [%]	58.66	67.92	53.25	58.72	68.12

Biomass conversion [%]	96.36	93.62	86.64	88.01	96.47
Cold gas efficiency [%]	69.78	84.41	65.33	74.83	87.40
Elutriated char [g_{daf}/ $kg_{biomass\ daf}$]	16.11	20.94	17.46	18.10	12.49
Elutriated fines [g/ $kg_{biomass\ daf}$]	60.78	82.39	61.54	62.30	61.82
Char generation [g_{daf}/ $kg_{biomass\ daf}$]	36.44	63.81	133.64	119.93	35.27
Ash generation (gasifier, cyclones and hot filter)[g_{db}/ $kg_{biomass\ daf}$]	59.74	93.69	130.19	106.32	72.17
Moisture generation [g/$kg_{biomass\ daf}$]	212.90	198.04	276.64	246.99	176.94
GC detectable tar [g/$kg_{biomass\ daf}$]	52.49	54.70	48.00	76.76	71.09

Table A2. Identified and quantified tar compounds.

			Magnesite		Olivine		
Tar compound	Retention time [min]	Tar group [Ref. Milne]	700 ºC [g/Nm^3]	800 ºC [g/Nm^3]	700 ºC [g/Nm^3]	760 ºC [g/Nm^3]	800 ºC [g/Nm^3]
Benzene	4.58	Secondary	0.76 ± 0.17	2.03 ± 0.81	5.11 ± 0.81	2.10 ± 0.43	3.45 ± 0.65
Toluene	7.89	Secondary	2.31 ± 0.50	3.28 ± 1.36	3.41 ± 0.45	4.94 ± 1.84	5.93 ± 0.50
Ethylbenzene	11.38	Secondary	0.19 ± 0.01	0.06 ± 0.00	0.12 ± 0.01	0.16 ± 0.02	0.06 ± 0.00
o/m/p-Xylene	11.70	Secondary	1.45 ± 0.05	1.01 ± 0.07	0.94 ± 0.09	2.28 ± 0.11	1.00 ± 0.09
Styrene	12.51	Secondary	1.35 ± 0.07	1.24 ± 0.11	1.01 ± 0.10	0.84 ± 0.04	1.60 ± 0.17
Indane	16.04	Secondary	3.39 ± 0.17	2.07 ± 0.24	2.13 ± 0.15	3.98 ± 0.29	1.98 ± 0.18
Phenol	16.27	Secondary	1.41 ± 0.10	1.13 ± 0.10	0.91 ± 0.05	2.13 ± 0.08	1.25 ± 0.10
Indene	17.90	Secondary	1.49 ± 0.11	2.33 ± 0.30	1.21 ± 0.11	3.03 ± 0.10	3.11 ± 0.35
o/m-Cresol	18.31	Secondary	3.34 ± 0.16	0.65 ± 0.04	1.58 ± 0.08	2.63 ± 0.16	0.47 ± 0.03
1,2-Dihydronaphthalene	21.16	Tertiary-PAH	0.47 ± 0.01	0.07 ± 0.00	0.25 ± 0.01	3.59 ± 1.43	0.06 ± 0.01
Naphthalene	22.29	Tertiary-PAH	2.10 ± 0.18	3.79 ± 0.57	1.68 ± 0.14	0.74 ± 0.03	5.24 ± 0.61
2-Methylnaphthalene	25.39	Tertiary-alkyl	1.14 ± 0.08	1.16 ± 0.14	0.79 ± 0.06	1.61 ± 0.04	1.35 ± 0.16
1-Methylnaphthalene	25.84	Tertiary-alkyl	0.60 ± 0.04	0.48 ± 0.06	0.42 ± 0.03	0.83 ± 0.02	0.59 ± 0.06
Acenaphthalene	29.45	Tertiary-PAH	0.59 ± 0.05	0.98 ± 0.16	0.47 ± 0.05	1.26 ± 0.04	1.43 ± 0.17
Fluorene	32.64	Tertiary-PAH	0.19 ± 0.02	0.38 ± 0.07	0.15 ± 0.02	0.41 ± 0.01	0.57 ± 0.07
Anthracene	36.87	Tertiary-PAH	0.35 ± 0.03	0.61 ± 0.11	0.25 ± 0.03	0.71 ± 0.04	0.86 ± 0.10
Fluoranthene	41.21	Tertiary-PAH	0.09 ± 0.01	0.17 ± 0.03	0.07 ± 0.01	0.20 ± 0.01	0.24 ± 0.02
Pyrene	41.91	Tertiary-PAH	0.10 ± 0.01	0.18 ± 0.03	0.08 ± 0.01	0.24 ± 0.02	0.26 ± 0.02
Benz[a]anthracene	45.87	Tertiary-PAH	0.06 ± 0.00	0.09 ± 0.01	0.04 ± 0.00	0.11 ± 0.01	0.10 ± 0.01
Total GC detectable			28.86 ± 0.94	26.97 ± 0.07	26.27 ± 2.13	42.80 ± 6.10	34.59 ± 1.75

Tar dew point* [ºC]			131.2	137.6	141.3	141.1	126.2

* Obtained from the ECN tar dew point site (www.thersites.nl)